

# TI Designs: TIDA-01236

## ワイヤレス超音波ガス漏えい検出器のコイン電池による動作時間を延長するリファレンス・デザイン



### 概要

このリファレンス・デザインでは、特定のシグネチャの超音波スペクトラムを分析してガスの漏えいを検出する、低消費電力のワイヤレス・センサを紹介します。このシステムは、単一のリチウム一次コイン電池で動作し、基地局とワイヤレスで通信するため、配線の要件が一切なく、簡単に設置できます。このデザインには超低消費電力のバッテリー残量ゲージが組み込まれており、バッテリーの状態を正確に予測して、バッテリーの寿命について前もって通知するため、バッテリーの交換をスケジュールできます。

### リソース

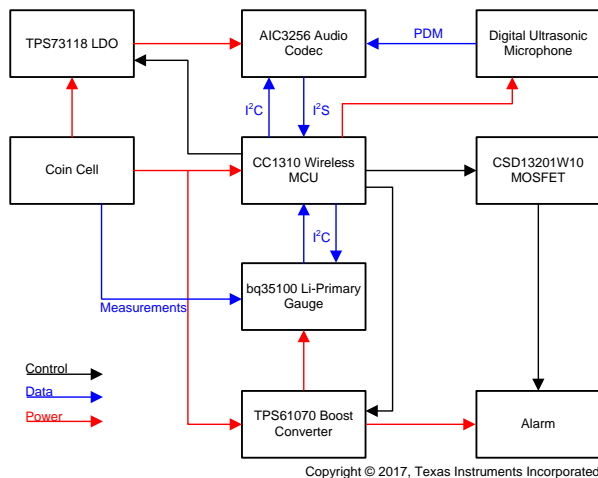
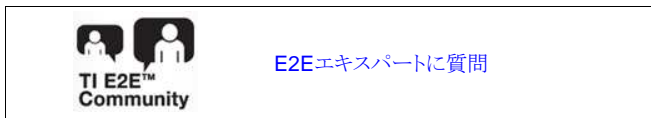
<a href="#">TIDA-01236</a>	デザイン・フォルダ
<a href="#">bq35100</a>	プロダクト・フォルダ
<a href="#">CC1310</a>	プロダクト・フォルダ
<a href="#">TLV320AIC3256</a>	プロダクト・フォルダ
<a href="#">TPS61070</a>	プロダクト・フォルダ
<a href="#">CSD13201W10</a>	プロダクト・フォルダ
<a href="#">TPS731</a>	プロダクト・フォルダ

### 特長

- リチウム一次バッテリーの正確な測定により、バッテリーの寿命を延長し、事前に保守可能
- 複数の電力ドメインを使用して、システムの消費電流を最適化
- システム診断により、開発中に正確な電力評価が可能
- 30秒ごとの測定を行う場合、コイン電池で3年以上動作
- ガスの種類にかかわらず漏えいを検出、センサ接触用のガスの濃縮は不要

### アプリケーション

- ガス検出
- ビルディング・オートメーション





使用許可、知的財産、その他免責事項は、最終ページにあるIMPORTANT NOTICE(重要な注意事項)をご参照くださいますようお願いいたします。英語版のTI製品についての情報を翻訳したこの資料は、製品の概要を確認する目的で便宜的に提供しているものです。該当する正式な英語版の最新情報は、[www.ti.com](http://www.ti.com)で閲覧でき、その内容が常に優先されます。TIでは翻訳の正確性および妥当性につきましては一切保証いたしません。実際の設計などの前には、必ず最新版の英語版をご参照くださいますようお願いいたします。

## 1 System Overview

### 1.1 System Description

Conventional gas-sensing approaches can entail a combination of wired gas sensor installations and manual inspection with a handheld unit. For locations that are impractical or expensive to reach with wired sensors, a wireless sensor installation is preferable to a periodic inspection, which requires an operator. However, traditional gas-sensing elements include a heating element to cause a measurable chemical reaction with the gas. These are not practical for long-term use on a system powered by a small battery due to their power consumption and preheat time. To achieve useful battery life, another sensing method must be employed.

Ultrasonic sensing is an attractive alternative that can be used in a duty-cycled system with low power consumption. Ultrasonic gas leak sensors do not detect the presence of a gas; rather, they detect the ultrasonic signature produced when a gas leaks from a pressurized pipe. Where a traditional chemical gas leak detector requires physical contact with a concentration of a particular type of gas for some period of time, an ultrasonic gas leak detector is not dependent on gas concentration and is capable of detecting any type of gas. Additionally, the audio-based detection mechanism enables efficient duty-cycling due to its instant on capability, which eliminates the preheating times of traditional sensors.

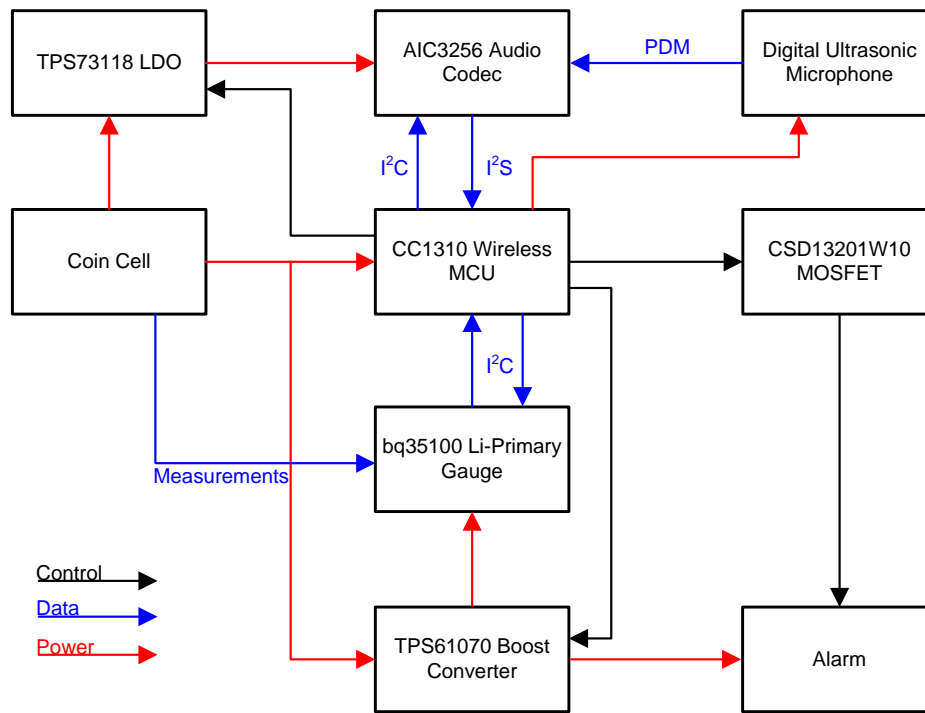
Designed as a replacement for a periodic manual inspection, this sensor wakes at a configurable interval (default 30 seconds) to check for leaks. This configuration enables wider coverage in a low-cost sensor that is easy to maintain. Each time the sensor wakes, it captures audio, performs a fast Fourier transform (FFT), analyzes the resulting frequency spectrum, and employs an algorithm to determine if a leak is present. If a leak is detected, the sensor wirelessly contacts a base station to report the leak and enable its onboard alarm. The sensor also wakes once per day to contact the base station and report its status and battery state.

### 1.2 Key System Specifications

表 1. Key System Specifications

PARAMETER	SPECIFICATIONS	DETAILS
Input power source	CR2477 Lithium-primary coin cell battery (3.0-V nominal voltage)	<a href="#">Section 1.5.1</a>
Average active-state current consumption ( $V_{IN} = 2.8\text{ V}$ )	4.18 mA	<a href="#">Section 2.2</a>
Active-state duration	119 ms	<a href="#">Section 2.2</a>
Average standby-state current consumption ( $V_{IN} = 2.8\text{ V}$ )	0.85 $\mu\text{A}$	<a href="#">Section 2.2</a>
Leak sense interval	30 s	<a href="#">Section 1.1</a>
Estimated battery life	Greater than three years	<a href="#">Section 2.2</a>
Leak detection range	Up to 8 m	<a href="#">Section 2.2</a>
Form factor	2.25- x 3.45- x 1.12-in rectangular PCB (57.15- x 87.63- x 28.45-mm)	<a href="#">Section 1.6</a>

### 1.3 Block Diagram



Copyright © 2017, Texas Instruments Incorporated

図 1. TIDA-01236 Simplified Block Diagram

### 1.4 Highlighted Products

#### 1.4.1 bq35100 Lithium Primary Battery Fuel Gauge and End-of-Service Monitor

The bq35100 Battery Fuel Gauge and End-Of-Service Monitor provides highly-configurable fuel gauging for non-rechargeable lithium primary batteries without requiring a forced discharge of the battery. Built so that optimization is not necessary, the patented TI gauging algorithms support replaceable batteries and enable accurate results with ultra-low average power consumption through host control through the GAUGE ENABLE (GE) pin.

The fuel gauging functions use voltage, current, and temperature information to provide State-of-Health (SoH) and End-of-Service (EOS) data. The bq35100 device only requires power for the duration of time that it takes to gather data and make the necessary calculations to support the selected algorithm and frequency of updates required by the system.

#### 1.4.2 CC1310 SimpleLink™ Sub-1 GHz Ultra-Low-Power Wireless Microcontroller

The CC1310 is a member of the CC26xx and CC13xx family of cost-effective, ultra-low-power, 2.4-GHz and sub-1 GHz RF devices. Very-low active RF and microcontroller (MCU) current consumption, in addition to flexible low-power modes, provide excellent battery lifetime and allow long-range operation on small coin cell batteries and in energy-harvesting applications.

The CC1310 device is the first device in a sub-1 GHz family of cost-effective, ultra-low-power wireless MCUs. The CC1310 device combines a flexible, very-low-power RF transceiver with a powerful 48-MHz Cortex®-M3 microcontroller in a platform which supports multiple physical layers and RF standards. A dedicated radio controller (Cortex®-M0) handles low-level RF protocol commands which are stored in ROM or RAM, thus ensuring ultra-low power and flexibility. The low-power consumption of the CC1310 device does not come at the expense of RF performance; the CC1310 device has excellent sensitivity and robustness (selectivity and blocking) performance.

The CC1310 device is a highly-integrated, true single-chip solution incorporating a complete RF system and an on-chip DC-DC converter. Sensors can be handled in a very low-power manner by a dedicated autonomous ultra-low-power MCU, which can be configured to handle analog and digital sensors; thus the main MCU (Cortex-M3) can maximize the sleep time.

The CC1310 power and clock management and radio systems require specific configuration and handling by software to operate correctly, which has been implemented in the TI-RTOS (TI real-time operating system for MCUs). TI recommends using this software framework for all application development on the device. The complete TI-RTOS and device drivers are offered in source code free of charge.

#### 1.4.3 TLV320AIC3256 Very-Low-Power Stereo Codec With miniDSP and DirectPath™ Stereo Headphone Amplifier

The TLV320AIC3256 (also called the AIC3256) is a flexible, low-power, low-voltage stereo audio codec with programmable inputs and outputs, PowerTune™ capabilities, fully-programmable miniDSP, fixed predefined and parameterizable signal processing blocks, integrated phase-locked loop (PLL), and flexible digital interfaces.

In this application, the TLV320AIC3256 captures audio from a digital microphone, performs decimation, and transfers the data to the host processor over an I<sup>2</sup>S interface. This approach offloads computationally-intensive decimation from the processor to the codec, which can perform this task much more efficiently. The TLV320AIC3256 supports multiple channels and integrates an audio amplifier. Using this same device, the designer can construct a more complex sensor architecture with multiple microphones to provide advanced filtering and directional information. The output channels can be used to generate a specific tone or play a recording for the alarm to differentiate from other sensors.

#### 1.4.4 TPS61070 Adjustable, 600-mA Switch, 90% Efficient PFM and PWM Boost Converter in Thin SOT-23

The TPS6107x devices provide a power supply solution for products powered by either a one-cell, two-cell, or three-cell alkaline, NiCd or NiMH, or one-cell Li-ion or Li-polymer battery. The boost converter is based on a fixed frequency, pulse-width-modulation (PWM) controller using a synchronous rectifier to obtain the maximum efficiency. At low load currents, the TPS61070 and TPS61073 enter the power-save mode to maintain a high efficiency over a wide load current range. The maximum peak current in the boost switch is typically limited to a value of 600 mA.

An external resistor divider programs the TPS6107x output voltage. The converter can be disabled to minimize battery drain. During shutdown, the load is completely disconnected from the battery. The device is packaged in a 6-pin thin SOT-23 package (DDC).

### 1.4.5 TPS731 Cap-Free, NMOS, 150-mA Low Dropout Regulator With Reverse Current Protection

The TPS731xx family of low-dropout (LDO) linear voltage regulators uses a new topology: an NMOS pass element in a voltage-follower configuration. This topology is stable using output capacitors with low equivalent series resistance (ESR) and even allows operation without a capacitor. The device also provides high reverse blockage (low reverse current) and ground pin current that is nearly constant over all values of output current.

The TPS731xx uses an advanced BiCMOS process to yield high precision while delivering very-low dropout voltages and low ground pin current. Current consumption, when not enabled, is less than 1  $\mu\text{A}$  and ideal for portable applications. These devices are protected by thermal shutdown and foldback current limit.

### 1.4.6 CSD13201W10 N-Channel NexFET™ Power MOSFET

This 12-V, 26-m $\Omega$ , N-Channel device is designed to deliver the lowest on resistance and gate charge in the smallest outline possible with excellent thermal characteristics in an ultra-low profile. The 0.8-V  $V_{GS(th)}$  voltage of the device can be easily interfaced to logic level IOs. In this application, the host processor directly controls the CSD13201W10 device to enable and disable the alarm.

## 1.5 Design Considerations

### 1.5.1 Power Management

#### 1.5.1.1 Battery Management

A 3-V 1000-mAh CR2477 LiMnO<sub>2</sub> coin cell powers the sensor. For reasons of efficiency, the system should run as long as possible before the user replaces the battery; however, it is more important that the system does not experience unexpected outages due to battery depletion. One approach is to measure the worst-case current consumption, calculate the runtime, and replace the battery with enough time in advance to avoid service interruptions. However, this approach leaves a significant portion of battery capacity unused after replacing the cell. Additionally, calculating the runtime is not a straightforward task in a complex system such as this, where the current consumption varies depending on the cell voltage, distance from the base station, temperature, leak detection interval, and many other factors.

To fully utilize the capacity of the battery and ensure predictable maintenance windows, this system utilizes the bq35100 battery fuel gauge for measurements and SoH predictions. The advanced gauging algorithm of the bq35100 device accounts for temperature variation, battery voltage, cell impedance, load current, and more in its determinations. Because the SoH is measured on a regular basis, the system can safely use more of the battery before it requires replacement. The system could also self-diagnose potential problems if the battery drains much faster than expected.

The extended runtime and SoH information provided by the gauge comes with virtually no increase to the system power consumption because the gauge can be so heavily duty-cycled. In this application, the gauge is enabled once per week for a few seconds to measure and recalculate the SoH. The expected system runtime is more than three years, so one week is well below 1% of the lifetime of the battery. Also, because the bq35100 reports the SoH in 1% increments, waking more than once per week is unnecessary. The designer can wirelessly change this interval during operation, if desired. See 2.2 for more details on power consumption.

Ensure that the battery is in a relaxed state when the bq35100 performs a measurement, as this step is important to prevent any recent significant discharge from affecting the battery voltage. LiMnO<sub>2</sub> batteries have a high internal impedance and a long time constant on transient effects. When a load is applied, the cell voltage drops due to its internal impedance. When the discharge ends, the battery voltage slowly recovers back to its open-circuit voltage level. For ideal results, the battery voltage must be at a stable, settled level when the gauge is enabled for measurement. Accomplish this stability by enabling the gauge after the longest OFF period of a duty-cycled system.

### 1.5.1.2 Alarm

The buzzer for this alarm has an integrated tone generator which emits sound whenever powered. The minimum 4-V operating voltage of this buzzer requires the use of a boost converter because the battery voltage range is 2 V to 3 V. The TPS61070 boost converter is chosen for its efficiency at light loads. To enable other components to share the output of the boost, this design uses the CSD12301W10 field-effect transistor (FET) to enable and disable the alarm. The 0.8-V  $V_{GS(TH)}$  of the FET is advantageous because it enables the general-purpose input and output (GPIO) from a CC1310 processor to directly control the alarm.

The boost converter also powers the bq35100 fuel gauge. The bq35100 RGIN and GE (gauge enable) pins are connected to the output of the boost converter and power the gauge whenever the boost converter is activated. In this scheme, the system can enable and disable the gauge using the lower-voltage boost enable signal.

### 1.5.1.3 Audio Codec

The TLV320AIC3256 audio codec requires a 1.8-V supply voltage, which the TPS731 LDO provides. The host processor disables this LDO when the codec is not in use to save power. Its dropout voltage is 30 mV at a 150-mA load, which is a much larger load than the codec will produce in this application. This low dropout voltage is an important factor because this system is designed to operate down to a 2-V battery level.

### 1.5.1.4 Firmware Considerations

The main processor and radio (CC1310) integrates a DC/DC converter to reduce its power consumption. The battery directly powers this converter because the CC1310 device is responsible for controlling the system timing and can put itself in shutdown mode when the battery is nearly depleted. The standby current of the CC1310 with a timer enabled is less than 1  $\mu$ A. The use of TI-RTOS in application firmware greatly simplifies power management; when properly configured, standby mode is automatically entered when all tasks are blocked and peripherals are not in use. The application firmware does not have to explicitly manage its own power states except when entering shutdown mode.

Because of the use of switching converters in this system, the overall current consumption increases as the battery voltage decreases. Managing this effect requires some care because LiMnO<sub>2</sub> coin cell batteries have a relatively high output impedance with a long time constant on transients. The firmware must avoid stacking these transient effects to minimize the worst-case transient load. For example, the boost converter causes a current spike when it powers on, which causes a voltage drop on the cell terminals. The firmware must also avoid doing a radio transmission during this time until the battery voltage recovers to prevent an early brownout.



Set the bq35100 max load parameter with the measured maximum system load at the system cutoff voltage. This step is important to enable the bq35100 device to correctly account for the internal voltage drop of the cell in SoH estimates at the end of the cell's life, where the lower voltage results in increased current consumption.

#### 1.5.1.5 *Diagnostic Mode*

The bq35100 saves power in SoH mode by initially performing all the required measurements and then completing the calculations afterwards. The bq35100 device can also be operated in an accumulator mode where, when enabled, it continuously measures and integrates current through a sense resistor. In this mode, the gauge must be enabled during system loads so that it can accurately track passed charge. Although the bq35100 is not designed to switch modes in the field, this system includes a diagnostic command for development use that switches the gauge into accumulation mode and enables current measurements. This mode is used to characterize the current consumption of various power modes for the sensor and quickly evaluate the impact of firmware changes on current consumption. A 1- $\Omega$  sense resistor is used to provide increased resolution in this mode. In a production setting, a sense resistor is not required for the bq35100 SoH mode, so the designer can replace this component with a 0- $\Omega$  resistor or a short.

## 1.5.2 Data Acquisition

As an ultrasonic gas leak sensor, this system requires some means of capturing ultrasonic audio. This design uses a digital microelectromechanical systems (MEMS) microphone with an 80-kHz bandwidth. The output of the microphone is a pulse-density modulated (PDM) stream that must be decimated for analysis. The TLV320AIC3256 audio codec supports digital microphones and is used to capture audio, digitally filter and downsample the signal to lower the sampling rate multi-bit data, and transmit the data back to the CC1310 processor over a digital I<sup>2</sup>S interface.

Care must be taken to ensure that the audio captured by the codec does not lose its ultrasonic information. Although the codec supports frequencies up to 192 kHz, its filters are designed for audio applications and have a 20-kHz bandwidth. The divider settings of the codec must be configured such that it increases the bandwidth of the filter. For a detailed description of the divider settings, see [TLV320AIC3256 Application Reference Guide](#). This application implements the following scheme:

The PRB\_7 codec processing block is used to select the decimation filter, which requires an oversampling rate (AOSR) of 64; thus, a MADC divider of 2 or higher is required. To accomplish this, a 24-MHz I<sup>2</sup>S MCLK is used as the main clock of the codec. The codec then samples from the digital microphone at a 12-MHz rate. However, the maximum clock frequency of the digital microphone is 4.8 MHz. Using the digital microphone clock output of the codec would violate the microphone specifications. To avoid this violation, a separate clock (CLKOUT) is generated by the codec from the 24-MHz MCLK with a divider of 8. This resulting 3-MHz clock is routed to the PDM clock input of the microphone. In this configuration, the codec will effectively zero-order hold the input data from the microphone until new data is available. Because the codec samples the microphone PDM stream faster than it is output, care must be taken to ensure the microphone data is not corrupted. The PDM format requires the microphone to tri-state its data signal when the clock level corresponds to the other channel. The design must ensure that the data driven by the microphone remains valid during the OFF period of the clock so that the codec reads this data correctly. After the microphone data has been captured, filtered, and downsampled by the codec, the resulting output is transmitted to the CC1310 as 16-bit, 187.5-kHz data.

## 1.5.3 Leak Detection

Pressurized gas leaks produce wideband ultrasonic noise that can be picked up by an ultrasonic microphone. This system uses a 1024-sample fixed-point FFT to analyze the frequency spectrum. The leak detection algorithm assumes that the background ultrasonic noise level remains stable. This assumption is based on measured results in the test environment. During initialization, the sensor captures the baseline ultrasonic noise level for each frequency bin by averaging multiple samples. The assumption is that no leaks are present when the sensor first powers on. A command to reset the baseline levels by re-measuring is included in the device firmware to enable adjustment if the background noise levels drift.

During operation, the sensor subtracts this baseline from the FFT samples to calculate a change in intensity. The change in intensity is then integrated across the 35-kHz to 65-kHz region and the result is compared against a threshold. If three consecutive samples are larger than the threshold, the sensor detects a leak. More elaborate filtering and detection algorithms can be developed using the same platform.



#### 1.5.4 Wireless Communication

The system minimizes power consumption by transmitting its status only once a day during normal conditions. When a leak is detected or stops being detected, the system immediately sends a notification to the base station. The radio is powered down for the remainder of the time, which means that the sensor cannot be used to retransmit packets in a mesh network. A star network topology with a single base station is used because it does not require the radio to stay on and requires the development of only one other node to use as a base station.

Whenever a sensor node sends a packet to the host, the node provides a window for the host to respond. The node retries a configurable amount of times before returning to normal operation to ensure that the host can receive the command if it is available. The host response signals the node to either return to normal operation or to await further commands. Although the host cannot communicate with the sensor during its OFF period, it will have an opportunity to communicate bidirectionally once per day or whenever a leak occurs. The user can configure a shorter communication rate, if necessary.

#### 1.5.5 Firmware Design

The system firmware has been developed, built, and programmed using TI's Code Composer Studio™ (CCS) software. The firmware uses TI-RTOS and leverages TI's CC1310 drivers whenever possible. A single task is able to efficiently meet the sensor requirements, so other tasks are not created. This single task maintains timers to control sensing, gauging, and RF communications.

To enable reuse and maintainability, sensor functionality is compartmentalized into modules. The individual subsystems are abstracted as devices such that the main code is not dependent on the hardware, operating system, or even physical implementation of the system. For example, the host communication system is implemented with packets transferred over a serial link. This serial link is supported by a wireless protocol but can be replaced by a serial port or other communication interface in another project. Similarly, each subsystem is supported by portable device drivers. These drivers implement communication to and control of hardware that fulfill subsystem functions. In turn, these drivers are built upon a set of CC1310 peripheral drivers. The application program interfaces (APIs) to these drivers can be implemented for another device if porting is required.

 2 shows the architecture of the sensor firmware.

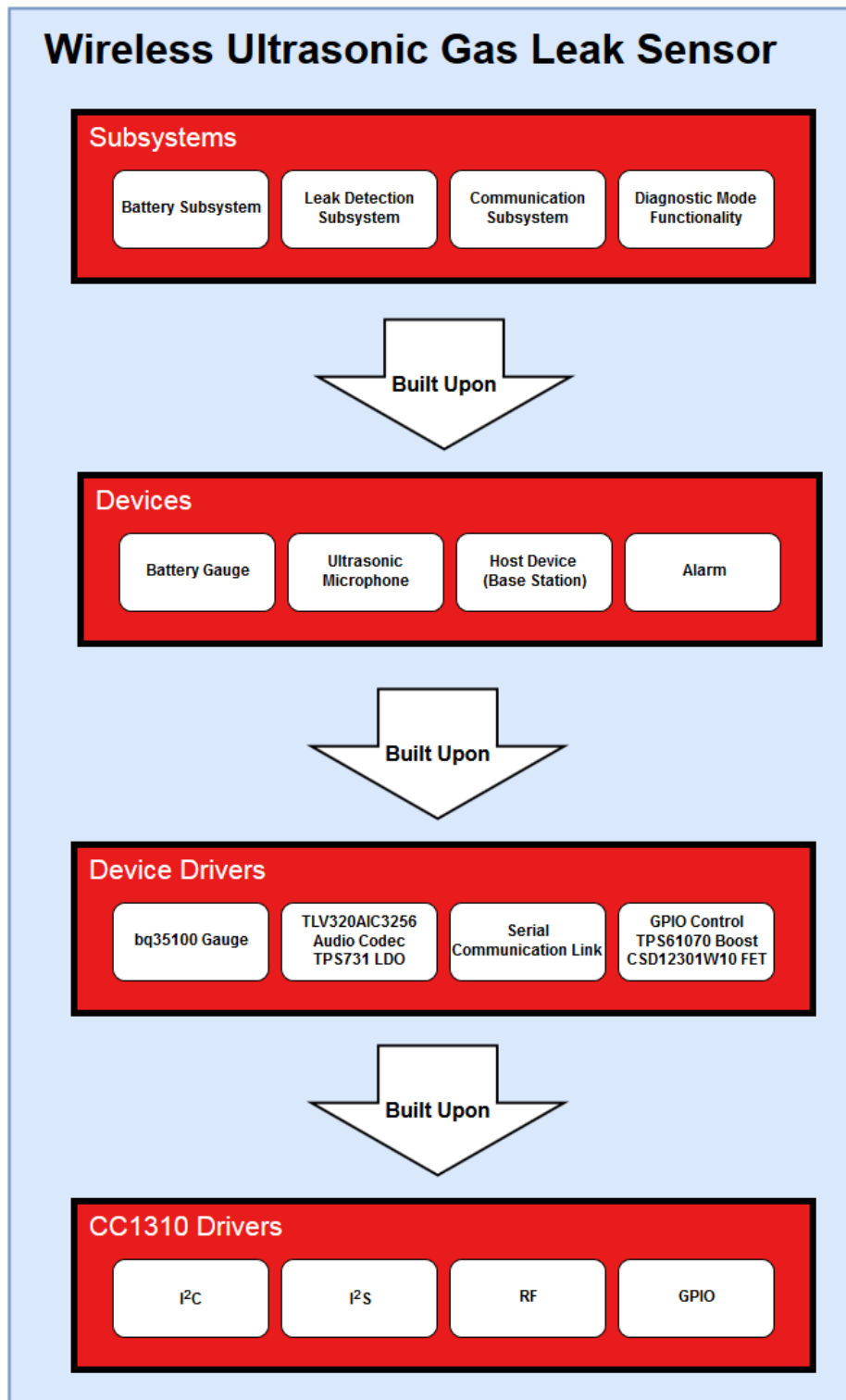
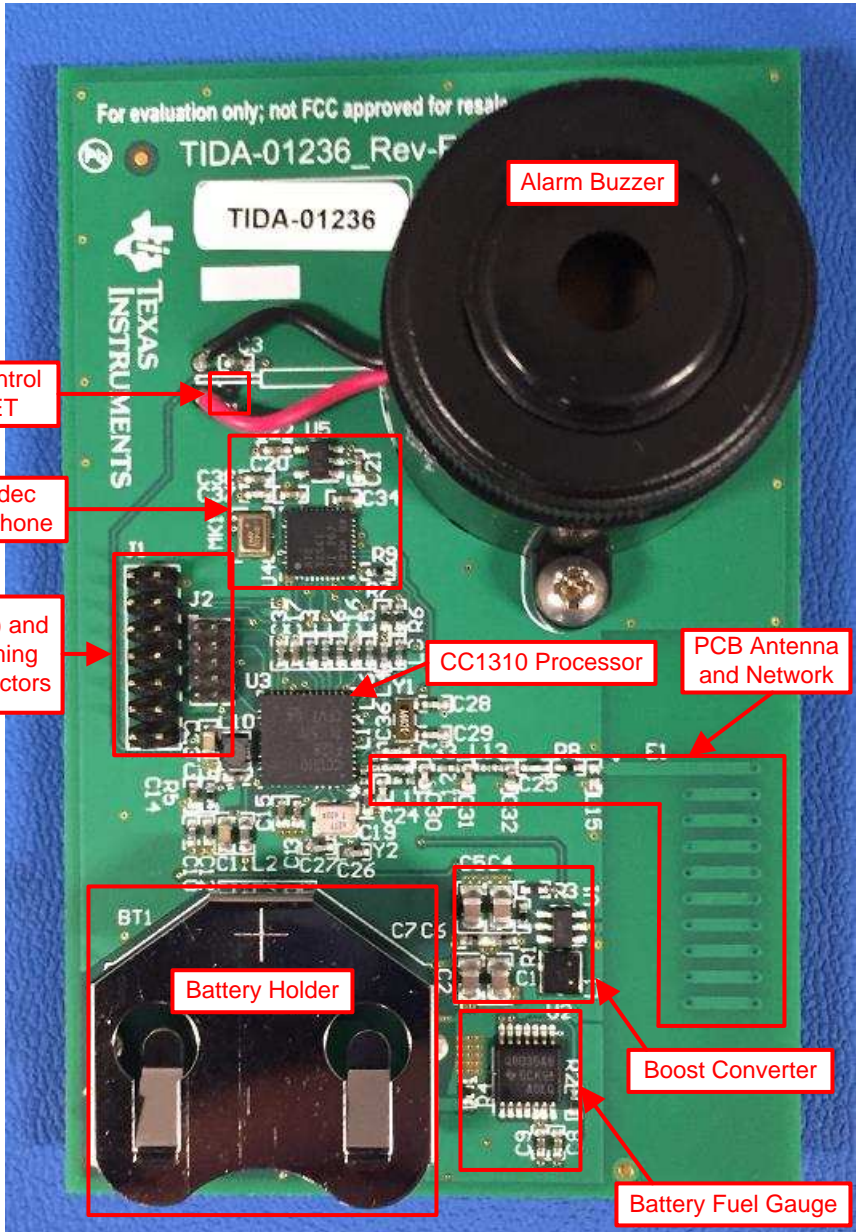
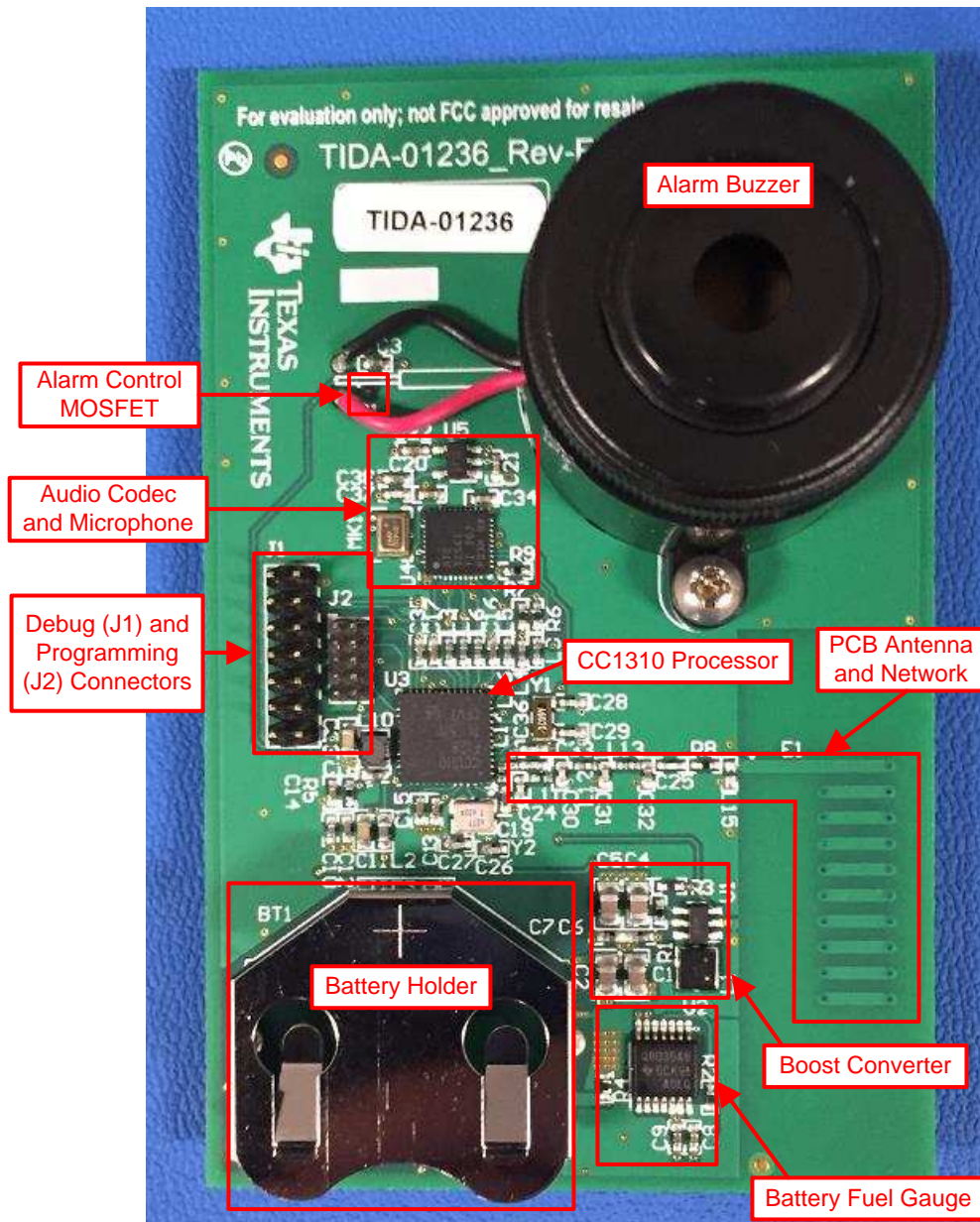


図 2. Firmware Architecture

### 1.6 PCB Design

The printed-circuit board (PCB) dimensions are 2.25 × 3.45 × 1.12 in (57.15 × 87.63 × 28.45 mm), which is primarily due to the decision to keep all components on the top side and to place the alarm buzzer on the board. This layout simplifies assembly and does not require external casing to hold the buzzer.  3 shows a diagram of the PCB component locations.

The large size of the buzzer, battery holder, and PCB antenna drives the overall shape of the board; other components are located around these. In a system where the buzzer is mounted to an enclosure and size is a concern, the designer can make the PCB smaller by moving the battery holder to the bottom side, using test points instead of the J1 debug header, and providing only connection points for the buzzer. With the space cleared by removing these components, the designer can then place the PCB antenna closer to the corner of the PCB.



**図 3. PCB Component Locations**

## 2 Testing and Results

System testing is separated into two categories: power consumption and leak detection. Because the sensor is duty-cycled with configurable intervals, the power consumption is measured for each of the sensor operational modes to enable accurate calculation of the overall power consumption and to enable the user to make informed decisions regarding the configuration settings.

### 2.1 Test Setup

A test leak apparatus was constructed as a stimulus for leak detection system testing (see [Figure 4](#)). This apparatus consists of a small pipe fitted with a pressure regulator, pressure gauge, ball valve, and a set of caps for the end of the pipe. A small hole was drilled in the end of each cap to simulate a repeatable leak (see [Figure 5](#)). This apparatus was then connected to a compressed air system. Given the directional nature of the simulated leak, all testing was performed with the leak directed toward the sensor.

The data was collected in a quiet room using the sensor in a diagnostic mode where it transmitted the raw audio, FFT output, and measured intensity to a PC for analysis. To filter out noise, ten audio samples were collected for each distance, pressure, and hole size. The average leak intensity of these ten samples was used in the following analysis.



**Figure 4. Test Leak Apparatus**



**Figure 5. Cap With Hole for Test Leak Apparatus**

Based on these results, the leak detection threshold was set at a relative leak intensity level of 500. Next, the detection range for the sensor at three different pressures was measured. This test was conducted in a large room in a lab with moderate background noise and various equipment in operation. A cap with a 0.53-mm diameter hole was connected to the test apparatus. After the sensor was powered on and had established a baseline for ambient noise, the test leak was activated. The sensor was then slowly moved away from the test apparatus until it no longer detected the leak and the distance was recorded. This test was repeated at three different pressures.

To measure system power consumption, the sensor firmware includes diagnostic commands to force it to enter specific operational modes for extended periods of time. These commands were used to cycle through the modes while measuring current consumption with a multimeter. Current consumption was measured at two different voltages. To enable average current calculations, the duration for each operation was also measured.

## 2.2 Test Results

Figure 6, Figure 7, and Figure 8 show the average leak intensity as recorded by the sensor with varied pressure, leak size, and distance from the sensor, respectively. Figure 9 shows the maximum leak detection distance with various air pressures at the test apparatus.

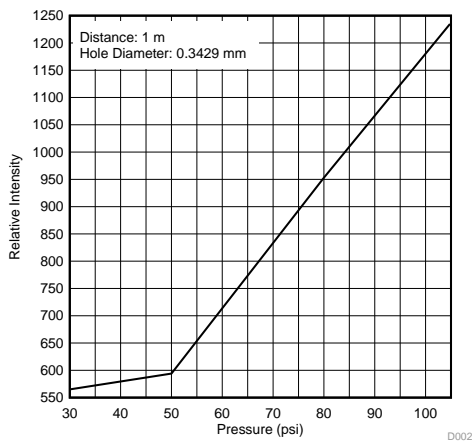


Figure 6. Relative Leak Intensity versus Pressure

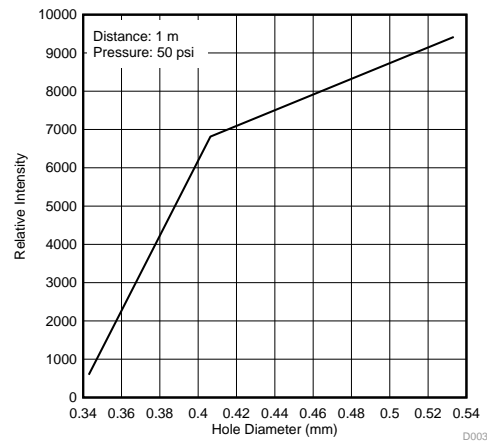


Figure 7. Relative Leak Intensity versus Hole Diameter

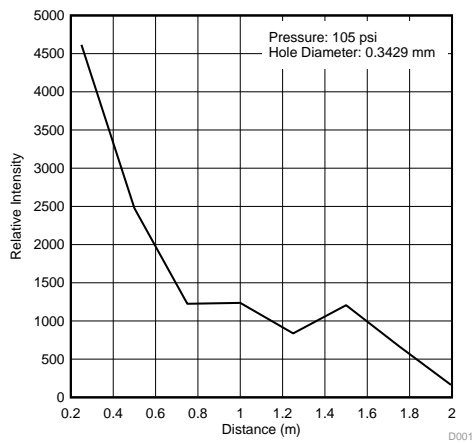


Figure 8. Relative Leak Intensity versus Distance

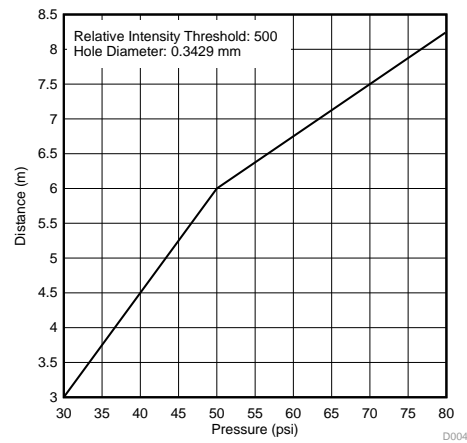


Figure 9. Maximum Leak Detection Distance versus Pressure

The active-mode current consumption ( $I_{ACTIVE}$ ) was measured at a 2.8- and 1.8-V system input voltage ( $V_{IN}$ ). Table 2 lists the duration and frequency of these operations along with the resulting calculated average current.

Table 2. Current Consumption

POWER MODE	$I_{ACTIVE}$ ( $V_{IN} = 2.8\text{ V}$ )	$I_{ACTIVE}$ ( $V_{IN} = 1.8\text{ V}$ )	DURATION	FREQUENCY	$I_{AVERAGE}$ ( $V_{IN} = 2.8\text{ V}$ )	$I_{AVERAGE}$ ( $V_{IN} = 1.8\text{ V}$ )
Audio capture	6.70 mA	5.85 mA	36 ms	30 s	8.04 $\mu\text{A}$	7.02 $\mu\text{A}$



**表 2. Current Consumption (continued)**

POWER MODE	$I_{ACTIVE} (V_{IN} = 2.8 V)$	$I_{ACTIVE} (V_{IN} = 1.8 V)$	DURATION	FREQUENCY	$I_{AVERAGE} (V_{IN} = 2.8 V)$	$I_{AVERAGE} (V_{IN} = 1.8 V)$
FFT calculation	3.09 mA	5.01 mA	83 ms	30 s	3.71 $\mu$ A	6.02 $\mu$ A
Radio RX	6.55 mA	10.73 mA	100 ms	1 wk	1.08 nA	1.77 nA
Radio TX	13.23 mA	21.71 mA	40 ms	1 wk	0.875 nA	1.44 nA
Gauge and boost on	123 $\mu$ A	140 $\mu$ A	2100 ms	1 wk	< 1 nA	< 1 nA
Sleep	0.85 $\mu$ A	1.30 $\mu$ A	—	—	0.85 $\mu$ A	1.30 $\mu$ A



## 3 Design Files

### 3.1 Schematics

To download the schematics, see the design files at [TIDA-01236](#).

### 3.2 Bill of Materials

To download the bill of materials (BOM), see the design files at [TIDA-01236](#).

### 3.3 PCB Layout Recommendations

Care should be taken to follow the layout guidelines of each individual component. This design uses four ground planes to minimize noise into sensitive parts of the system. The microphone and codec are each located on their own respective planes to minimize noise into the audio signal. The boost converter is kept on its own plane to keep its noise out of the rest of the system. The boost layout uses short traces wherever possible to minimize electromagnetic interference (EMI) from switching. The gauge is also on its own plane to keep its measurements clean even when other parts of the system are active. The traces to the sense resistor are routed as a differential pair to minimize noise. TI recommends a filter network for the sense resistor in applications where accurate current measurements are more critical. For more details, see [bq35100 Lithium Primary Battery Fuel Gauge and End-Of-Service Monitor](#).

#### 3.3.1 Layout Prints

To download the layer plots, see the design files at [TIDA-01236](#).

### 3.4 Altium Project

To download the Altium project files, see the design files at [TIDA-01236](#).

### 3.5 Gerber Files

To download the Gerber files, see the design files at [TIDA-01236](#).

### 3.6 Assembly Drawings

To download the assembly drawings, see the design files at [TIDA-01236](#).

## 4 Software Files

To download the software files, see the design files at [TIDA-01236](#).

## 5 Related Documentation

1. Texas Instruments, [bq35100 Technical Reference Manual](#)
2. Texas Instruments, [TLV320AIC3256 Application Reference Guide](#)
3. Texas Instruments, [CC13x0, CC26x0 SimpleLink™ Wireless MCU Technical Reference Manual](#)
4. Texas Instruments, [CC26x0, CC13x0 SimpleLink™ Wireless MCU Power Management Software Development Reference Guide](#)

## 5.1 商標

SimpleLink, DirectPath, PowerTune, NexFET, Code Composer Studio are trademarks of Texas Instruments.

Cortex is a registered trademark of Arm Limited.

すべての商標および登録商標はそれぞれの所有者に帰属します。

## 6 About the Author

**MICHAEL O'BRIEN** is a firmware engineer at Texas Instruments, where he is responsible for developing firmware for battery fuel gauge products. Michael has experience with software and embedded system design. He earned his bachelor of science (BS) in engineering with an electrical concentration from Oral Roberts University in Tulsa, Oklahoma.

## TIの設計情報およびリソースに関する重要な注意事項

Texas Instruments Incorporated ("TI")の技術、アプリケーションその他設計に関する助言、サービスまたは情報は、TI製品を組み込んだアプリケーションを開発する設計者に役立つことを目的として提供するものです。これにはリファレンス設計や、評価モジュールに関係する資料が含まれますが、これらに限られません。以下、これらを総称して「TIリソース」と呼びます。いかなる方法であっても、TIリソースのいずれかをダウンロード、アクセス、または使用した場合、お客様(個人、または会社を代表している場合にはお客様の会社)は、これらのリソースをここに記載された目的にのみ使用し、この注意事項の条項に従うことに合意したものとします。

TIによるTIリソースの提供は、TI製品に対する該当の発行済み保証事項または免責事項を拡張またはいかなる形でも変更するものではなく、これらのTIリソースを提供することによって、TIにはいかなる追加義務も責任も発生しないものとします。TIは、自社のTIリソースに訂正、拡張、改良、およびその他の変更を加える権利を留保します。

お客様は、自らのアプリケーションの設計において、ご自身が独自に分析、評価、判断を行う責任がお客様にあり、お客様のアプリケーション(および、お客様のアプリケーションに使用されるすべてのTI製品)の安全性、および該当するすべての規制、法、その他適用される要件への遵守を保証するすべての責任をお客様のみが負うことを理解し、合意するものとします。お客様は、自身のアプリケーションに関して、(1) 故障による危険な結果を予測し、(2) 障害とその結果を監視し、および、(3) 損害を引き起こす障害の可能性を減らし、適切な対策を行う目的での、安全策を開発し実装するために必要な、すべての技術を保持していることを表明するものとします。お客様は、TI製品を含むアプリケーションを使用または配布する前に、それらのアプリケーション、およびアプリケーションに使用されているTI製品の機能性を完全にテストすることに合意するものとします。TIは、特定のTIリソース用に発行されたドキュメントで明示的に記載されているもの以外のテストを実行していません。

お客様は、個別のTIリソースにつき、当該TIリソースに記載されているTI製品を含むアプリケーションの開発に関連する目的でのみ、使用、コピー、変更することが許可されています。明示的または黙示的を問わず、禁反言の法理その他どのような理由でも、他のTIの知的所有権に対するその他のライセンスは付与されません。また、TIまたは他のいかなる第三者のテクノロジーまたは知的所有権についても、いかなるライセンスも付与されるものではありません。付与されないものには、TI製品またはサービスが使用される組み合わせ、機械、プロセスに関連する特許権、著作権、回路配置利用権、その他の知的所有権が含まれますが、これらに限られません。第三者の製品やサービスに関する、またはそれらを参照する情報は、そのような製品またはサービスを利用するライセンスを構成するものではなく、それらに対する保証または推奨を意味するものでもありません。TIリソースを使用するため、第三者の特許または他の知的所有権に基づく第三者からのライセンス、もしくは、TIの特許または他の知的所有権に基づくTIからのライセンスが必要な場合があります。

TIのリソースは、それに含まれるあらゆる欠陥も含めて、「現状のまま」提供されます。TIは、TIリソースまたはその仕様に関して、明示的か暗黙的にかかわらず、他のいかなる保証または表明も行いません。これには、正確性または完全性、権原、続発性の障害に関する保証、および商品性、特定目的への適合性、第三者の知的所有権の非侵害に対する黙示的保証が含まれますが、これらに限られません。

TIは、いかなる苦情に対しても、お客様への弁済または補償を行う義務はなく、行わないものとします。これには、任意の製品の組み合わせに関連する、またはそれらに基づく侵害の請求も含まれますが、これらに限られず、またその事実についてTIリソースまたは他の場所に記載されているか否かを問わないものとします。いかなる場合も、TIリソースまたはその使用に関連して、またはそれらにより発生した、実際の、直接的、特別、付随的、間接的、懲罰的、偶発的、または、結果的な損害について、そのような損害の可能性についてTIが知らされていたかどうかにかかわらず、TIは責任を負わないものとします。

お客様は、この注意事項の条件および条項に従わなかったために発生した、いかなる損害、コスト、損失、責任からも、TIおよびその代表者を完全に免責するものとします。

この注意事項はTIリソースに適用されます。特定の種類の資料、TI製品、およびサービスの使用および購入については、追加条項が適用されます。これには、半導体製品(<http://www.ti.com/sc/docs/stdterms.htm>)、評価モジュール、およびサンプル(<http://www.ti.com/sc/docs/sampterms.htm>)についてのTIの標準条項が含まれますが、これらに限られません。